Statistical evaluation of outdoor-to-indoor office MIMO measurements at 5.2 GHz

Wyne, Shurjeel; Molisch, Andreas; Almers, Peter; Eriksson, Gunnar; Kåredal, Johan; Tufvesson, Fredrik

Published in:
2005 IEEE 61st Vehicular Technology Conference

DOI:
10.1109/VETECS.2005.1543267

2005

Statistical Evaluation of Outdoor-to-Indoor Office MIMO Measurements at 5.2 GHz

Shurjeel Wyne[1], Andreas F. Molisch[1,2], Peter Almers[1,3], Gunnar Eriksson[1,4], Johan Karedal[1], and Fredrik Tufvesson[1]

[1]Dept. of Electroscience, Lund University, Box 118, SE-221 00 Lund, Sweden

[2]Mitsubishi Electric Research Labs, 201 Broadway, Cambridge, MA 02139, USA

[3]TeliaSonera AB, Box 94, SE-201 20 Malmö, Sweden

[4]Swedish Defence Research Agency, Box 1165, SE-581 11 Linköping, Sweden

E-mail: Firstname.Lastname@es.lth.se

***Abstract*— In this paper, we present a statistical evaluation of an outdoor-to-indoor Multiple-Input Multiple-Output (MIMO) measurement campaign performed at 5.2 GHz. 159 measurement locations in an office building are analyzed. Our analysis pays special attention to two key assumptions that are widely used in stochastic channel models. An assumption that is used in practically every channel model is that the channel can be represented as a sum of a line-of-sight (LOS) component plus a (possibly correlated) zero-mean complex Gaussian distribution. Our investigation shows that this model does NOT adequately represent our measurement data. Our analysis also highlights the difference between the LOS power factor and the Ricean K-factor. We show that the direction-of-arrival (DOA) spectrum depends noticeably on the direction-of-departure (DOD). Therefore, the popular Kronecker model is not applicable, and the more general Weichselberger model should be used.**

***Index Terms*—MIMO, DOA, DOD, LOS power factor, Ricean K-factor, Kronecker model, Weichselberger model.**

I. Introduction

Multiple antennas at both receiver and transmitter can result in tremendous capacity improvements over single antenna systems [1]. Ultimately, the capacity gains depend on the propagation channel in which the system is operating. The establishment of good channel models is also essential both for the development of new algorithms for signal processing, modulation and coding, and for the unified testing of different system proposals in standardization. The two hallmarks of a good channel model are (i) simplicity, and (ii) agreement with reality.

There are two main categories of channel models for MIMO systems:

1) double-directional channel models [2], which describe the parameters of multipath components DOD, DOA, delay, and complex amplitudes. Such models are highly useful because they are independent of antenna configurations and describe the physical propagation alone.
2) analytical channel models, which describe the statistics of the transfer function matrix; each entry in that matrix gives the transfer function from the i-th transmit to the j-th receive antenna element. Note that it is easy to obtain an analytical channel model from a double-directional model but not the other way around.

All of the analytical models are based on the assumption that the entries of the transfer function matrix are zero-mean complex Gaussian, with the possible addition of a line-of-sight component. Furthermore, many models describe the correlation matrix of those entries as a Kronecker product of the correlation matrices at the transmit and receive side. The first assumption has, to our knowledge, generally remained unquestioned[1]. The Kronecker assumption has been discussed more extensively recently [5], [6]. While measurement data from outdoor scenarios seem to indicate good agreement with this assumption [5], indoor data seem to deviate more [6], and as a consequence, a more general model has been developed by Weichselberger et al. [7].

In this paper, we present a statistical analysis of the results of a recent measurement campaign [8], and compare it to those popular models. Our main contributions are

- we investigate the validity of the LOS-plus-Gaussian-remainder assumption, and show that it does not hold for all measurement locations in our campaign.
- we explain this result by investigating in detail the difference between "LOS power factor" and "Ricean K-factor".
- we analyze the validity of the Kronecker model, and present detailed results on the coupling between DOAs and DODs.

II. Measurement setup

The measurement setup is described in detail in [8] and summarized here for the convenience of the reader. Measurement data were recorded with the RUSK ATM channel sounder. The measurements were performed at a center frequency of 5.2 GHz and a signal bandwidth of 120 MHz. The transmit antenna was an 8 element dual polarized uniform linear patch array with element spacing $\approx \lambda/2$. The receive antenna was a 16-element uniform circular array with vertically polarized monopole elements, radius $\approx \lambda$. This array had an absorber in the middle as shown in right half of Fig. 1. The measurement results directly give the channel transfer function matrix; however, for some aspects of our investigation (LOS analysis), we needed the multipath component (MPC) parameters. Those were obtained with the high-

[1] with the exception of the rare "keyhole scenario", see [3], [4].

Fig. 1. An 8-element dual polarized uniform linear patch array was used at the transmit side and a 16-element vertically polarized uniform circular array was used at the receive side.

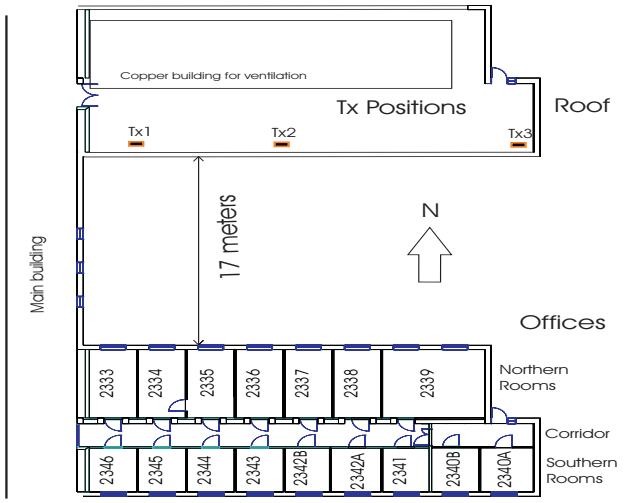

Fig. 2. Site map showing locations of Tx (3rd floor) and Rx positions (2nd floor). The free space distance between the blocks is also indicated. 4-7 positions were measured in room: 2334, 2336, 2337,2339 (referred to as north) and 2345, 2343, 2342A, 2340B (referred to as south).

resolution SAGE algorithm [9]; only the 8 vertically polarized elements on the transmit array were considered for this analysis.

The test site is the E building at LTH, Lund University, Sweden. The site map is shown in Fig. 2. The transmitter was placed at 3 different positions on the roof of a nearby building. For each transmit position, the receiver was placed at 53 measurement positions spread over 8 different rooms and the corridor.

III. Results

A. Fading Statistics of Channel Coefficients

It is well known that in a measured scenario where a LOS component is present, the channel coefficients have a non-zero mean complex Gaussian distribution. Consequently, the measured channel matrix may be modeled as the weighted sum of an estimated LOS (deterministic part) and a zero mean complex Gaussian distributed residue component [10]

$$\begin{aligned}\mathbf{H}_{\text{model}} &= \sqrt{\frac{K_{\text{LOS}}}{K_{\text{LOS}}+1}}\hat{\mathbf{H}}_{\text{LOS}} + \sqrt{\frac{1}{K_{\text{LOS}}+1}}\hat{\mathbf{H}}_{\text{res}} \\ &= \sqrt{\frac{K_{\text{LOS}}}{K_{\text{LOS}}+1}}\hat{\mathbf{H}}_{\text{LOS}} + \sqrt{\frac{1}{K_{\text{LOS}}+1}}\text{un-vec}\left\{\hat{\mathbf{R}}^{1/2}\mathbf{G}\right\},\end{aligned} \tag{1}$$

where the estimate of the channel correlation matrix $\hat{\mathbf{R}}$ is computed as

$$\hat{\mathbf{R}} = \frac{1}{M}\sum_{\mathbf{m=1}}^{\mathbf{M}} \text{vec}\left\{\hat{\mathbf{H}}_{\text{res}}(m)\right\}\text{vec}\left\{\hat{\mathbf{H}}_{\text{res}}(m)\right\}^{H}. \tag{2}$$

$\hat{\mathbf{H}}_{\text{LOS}}$ is the estimated and normalized contribution to the channel matrix by the LOS component. $\hat{\mathbf{H}}_{\text{res}}(m)$ is the estimated residue part in the m :th channel matrix realization, $\mathbf{G}$ is a random matrix with i.i.d. zero-mean complex Gaussian entries. Further vec$\{\cdot\}$ is the vector operator that stacks the columns of a matrix on top of each other, un-vec$\{\cdot\}$ is the inverse operation. This modeling approach of a Ricean measured channel with a Gaussian residue component did not fully fit our measuremet data. Fig. 3 demonstrates an exemplary case where the magnitudes of the channel coefficients, in a measured LOS scenario, do not exhbit a Ricean distribution. The PDF was computed from the data for one measurement location, such that both spatial realizations and the 193 frequency sub-channels constituted the sample function. On further analysis of the LOS scenarios, it was revealed that some elements of the Rx aray were suffering from shadow fading, i.e., the mean channel power at the elements of the Rx array, averaged over all frequencies and Tx elements, varied considerably over the array. This shadowing was due to the absorber placed in the center of the circular array. We conjecture that a similar effect would be found with a circular array of patch antennas. The possibility that the shadowing resulted from the Rx array being partially located within the first fresnel zone of the vertical window edge was also studied but dis-regarded after cross-checking the relevant Rx positions on the measurement map. Figs. 5, 6 illustrate how the absorber attenuates the LOS signal received at the back elements of the Rx array. Hence the overall fading distribution of the channel coefficients is affected by which Rx elements are considered for the ensemble. In an attempt to fit various theoretical PDFs to the LOS measurement data, we found that the Generalized Gamma distribution [11], [12] best represented our measured channel. The distribution is given as [11]

$$\begin{aligned}p_{GG}(r) &= \frac{cr^{(c\alpha-1)}}{\beta^{c\alpha}\Gamma(\alpha)}e^{-\left(\frac{r}{\beta}\right)^{c}} \\ \beta &= \sqrt{E[r^2]\frac{\Gamma(\alpha)}{\Gamma\left(\frac{c\alpha+2}{c}\right)}}\end{aligned} \tag{3}$$

where α, β, and c are the distribution parameters and $\Gamma(\cdot)$ is the Gamma function. When characterizing a channel with Eq. (3) the lower tail shape of the PDF is determined by $c\alpha - 1$ and the upper tail by c. For all LOS scenarios that were analyzed, the theoretical PDF provided a good fit to the measured data with

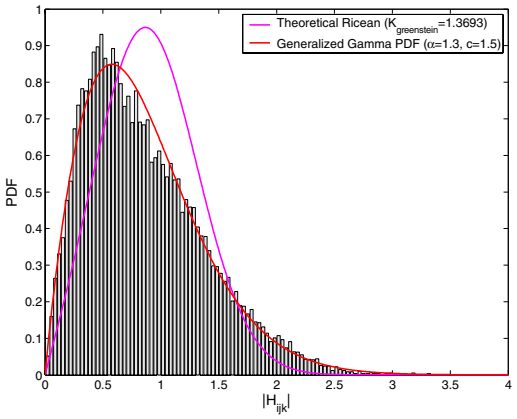

Fig. 3. G. Gamma PDF fit to measured data histogram. Position Tx1Rx2334ME.

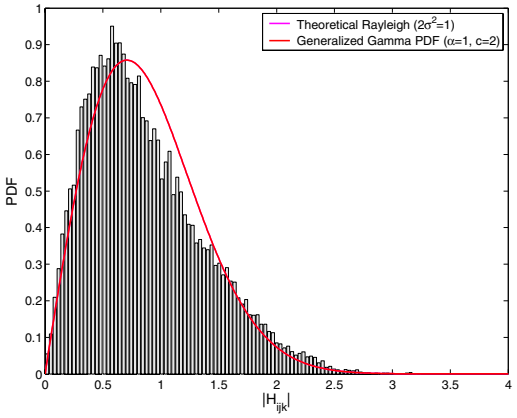

Fig. 4. G. Gamma PDF fit to data histogram for residue channel. Position Tx1Rx2334ME.

α in the range $1.2 - 3.5$ and c in the range $0.7 - 1.6$. For the residue channel as well as NLOS scenarios, the parameter values $c = 2$, $\alpha = 1$, corresponding to a Rayleigh fading statistic [12], provided a good match to the data histogram. Figs. 3, 4 compare PDF fits to measured data for a typical LOS position. As an important consequence of our investigation, we thus find that the "standard" model might not be universally applicable and that shadowing due to certain array configurations can distort the fading statistics. On an explanatory note, Eq. (1) may be misleading in the sense that one would expect an ensemble of measured MIMO channel matrices in a LOS scenario to have a non-zero mean. However, measured channels with a Ricean component can have zero mean. This is possible, e.g., when the channel matrices at different frequency sub-channels are treated as separate channel realizatons, due to the phase-shift associated with different realizations, complex addittion can result in a matrix with zero mean.

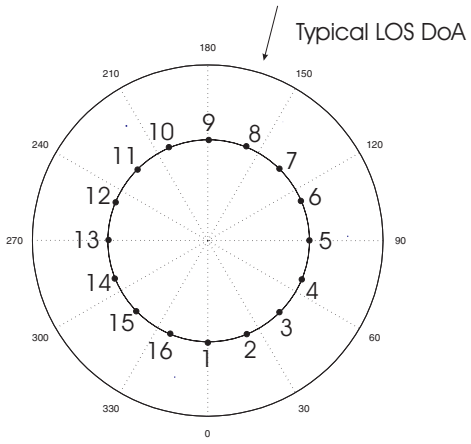

Fig. 5. Orientation of UCA elements w.r.t estimated DOAs. Angle measure (0-360°) and element numbers (1-16) indicated along circumference of UCA.

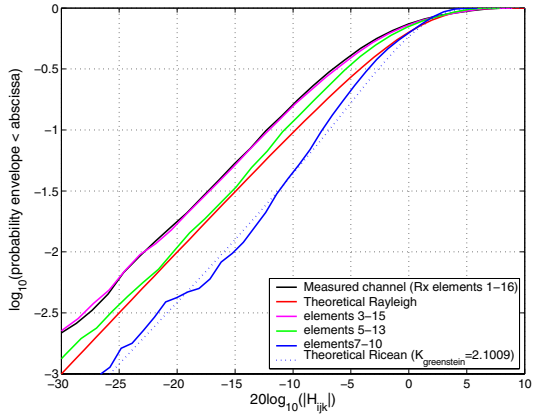

Fig. 6. Measured channel: Effect of selecting Rx elements on the fading distribution of the channel coefficients. Position Tx2Rx2336NM

B. LOS power factor and Ricean K-factor

The LOS power factor $K_{LOS} = \dfrac{E\left[\left\|\hat{\mathbf{H}}_{\text{LOS}}\right\|_F^2\right]}{E\left[\left\|\hat{\mathbf{H}}_{\text{res}}\right\|_F^2\right]}$, extracted from measurements (un-normalized matrices), was used in modeling LOS scenarios according to Eq. (1), where $\|\cdot\|_F$ denotes Frobenius norm of it's matrix argument. The LOS estimate $\hat{\mathbf{H}}_{\text{LOS}}$ can be obtained from a high resolution algorithm, such as SAGE, by inserting channel parameters of the LOS path into the signal model assumed by the algorithm.

It must be stressed that this "LOS power factor" is different from the Ricean K-factor. The LOS power factor relates physically to the line-of-sight component, which is strong, but not necessarily the only strong component. Still, it can be uniquely identified in a MIMO scenario by its DOA, DOD (they have to agree with the angles that correspond to the "direct line" between transmitter and receiver), and the delay, which is the smallest of all multipath components. The Ricean K-factor, on the other hand, is a characteristic parameter of the amplitude distribution. It is conventionally related to the *narrowband* amplitude distribution;

TABLE I

Comparison of LOS power factor and Ricean K-factor.

Position	Rx elements	K_{LOS}	K_{rice}
Tx1 Rx2334ME	8-11	0.93	1.08
Tx1 Rx2334MM	8-11	2.47	4.28
Tx2 Rx2336NM	7-10	2.23	2.10
Tx2 Rx2336MW	8-11	5.74	4.16
Tx2 Rx2337ME	9-12	2.83	3.03

even when it is used to describe the amplitude characteristics of the first delay bin, it does not have a strict correspondence to the LOS component. Ricean K-factors can be extracted, e.g., with the method-of-moments as suggested by Greenstein [13]. Table 1 compares the Rice factors and LOS power factors in some of our measurement locations. Since the shadowing effect from the UCA absorber distorts the fading statistics when the full Rx array is considered, a subset of 4 Rx elements was selected, which form an arc subtending an angle $\approx 67^\circ$ at the center of the array, and contain the DOA of the LOS MPC. The evaluation of the LOS power factor and the Ricean K-factor has been done for the subset elements. The results shown in Table 1 indicate a general trend that the LOS power factor is less than or similar to the Ricean K-factor. The strong exception is at the position Tx2Rx2336MW, where the LOS power factor is much stronger than the Ricean K-factor. However no explanation could be determined for this behaviour.

C. Inter-connection between DOAs and DODs

As a third topic of our investigation, we analyze the correlation between DOAs and DODs. 40 MPCs were extracted at each measured location using the SAGE algorithm. In Fig. 7 the joint DOA-DOD spectrum is shown for some Rx positions corresponding to Tx position 1. The plot shows that specific DODs are linked to specific DOAs such that the joint spectrum is not separable into the marginal spectrums. To quantify this effect, we investigate two analytical channel models that make different assumptions about the coupling between DOAs and DODs.

1) Kronecker model: The Kronecker model [5], [14] generates a correlated Rayleigh fading channel matrix as in Eq. (1) but approximates the full channel correlation matrix $\mathbf{R}$ by the Kronecker product of the transmit and receive antenna correlation matrices; $\mathbf{R}_{\text{Tx}}$ and $\mathbf{R}_{\text{Rx}}$ respectively.

$$\hat{\mathbf{R}} = \frac{1}{tr\{\hat{\mathbf{R}}_{\text{Rx}}\}} \hat{\mathbf{R}}_{\text{Tx}} \otimes \hat{\mathbf{R}}_{\text{Rx}}, \tag{4}$$

where

$$\hat{\mathbf{R}}_{\text{Rx}} = \frac{1}{M} \sum_{m=1}^{M} \mathbf{H}(m)\, \mathbf{H}(m)^H, \tag{5}$$

$$\hat{\mathbf{R}}_{\text{Tx}} = \frac{1}{M} \sum_{m=1}^{M} \mathbf{H}(m)^T\, \mathbf{H}(m)^*. \tag{6}$$

$tr\{\cdot\}$ represents trace of a matrix and $(\cdot)^*$ represents complex conjugate. $\mathbf{H}(m)$ is one of M channel realizations. According to the Kronecker asumption, the same DOA spectrum and hence Rx correlation matrix will be produced irrespective of the DOD and vice versa. According to [6] the Kronecker underestimates the channel capacity. We analyzed the validity of the Kronecker model for various antenna arrangements and measurement locations. For the LOS scenarios, we are limited to a subset of the receive array to prevent distortion of fading statistics, hence channel matrices of small rank. Fig. 8 shows the modeled capacity plotted against the measured one for a number of measurement locations. The Kronecker model deviates only very little from the measured results for a 2x8 setup. For NLOS scenarios (Fig. 9), the larger 16x8 setup shows greater deviations between the modeled and measured capacity as explained in [15]. The measured SNR at the NLOS positions was in the range of 1-10 dB, hence the same was used as the evaluation SNR. Since noise has a Kronecker structure, the model will match 'measured' capacity better at lower capacities (small SNR) as observed in Fig 9.

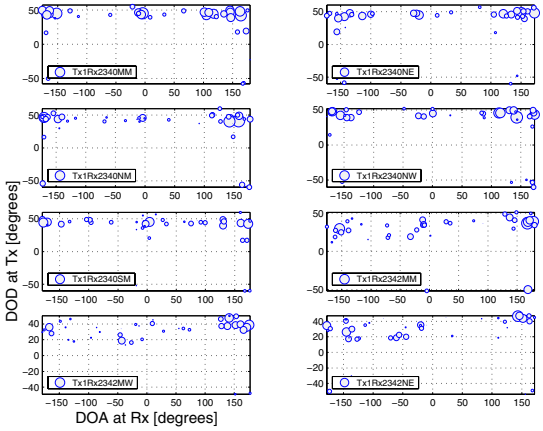

Fig. 7. Joint DOA DOD plot for the South rooms, Tx position 1. Marker size is scaled relative to power of the strongest component [dB scale].

2) Weichselberger Model: The Weichselberger model [7] is less restrictive than the Kronecker model in that it allows for any arbitrary coupling between the transmit and receive eigenbases, the only requirement is that the eigenbasis at Rx is independent of DOD and vice versa. The channel is modeled as [7]

$$\hat{\mathbf{H}}_{weichsel} = \hat{\mathbf{U}}_{\text{Rx}} \left(\tilde{\Omega} \odot \mathbf{G} \right) \hat{\mathbf{U}}_{\text{Tx}}^T, \tag{7}$$

where the operator $\odot$ denotes element-wise Schur-Hadamard product, $\hat{\mathbf{U}}_{\text{Rx}}$ and $\hat{\mathbf{U}}_{\text{Tx}}$ are the estimated receive and transmit eigenbasis given by the eigenvalue decomposition of the respective antenna correlation matrices, $\mathbf{G}$ is a random fading matrix with i.i.d. complex Gausian entries, and $\tilde{\Omega}$ is the element-wise square root of the power coupling matrix Ω. The i, j :th entry of the power coupling matrix gives the average power coupled between the i :th receive and j :th transmit eigenmode, the matrix is estimated as

$$\hat{\Omega} = \frac{1}{M} \sum_{m=1}^{M} \left[\left(\hat{\mathbf{U}}_{\text{Rx}}^H \mathbf{H}(m)\, \hat{\mathbf{U}}_{\text{Tx}}^* \right) \odot \left(\hat{\mathbf{U}}_{\text{Rx}}^T \mathbf{H}(m)^*\, \hat{\mathbf{U}}_{\text{Tx}} \right) \right] \tag{8}$$

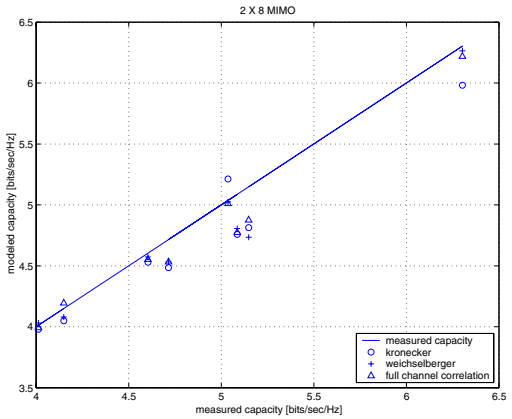

Fig. 8. LOS, 2x8 MIMO; Scatter plot of average model capacity against average capacity of measured channel. The identity line indicates points of no modeling error.

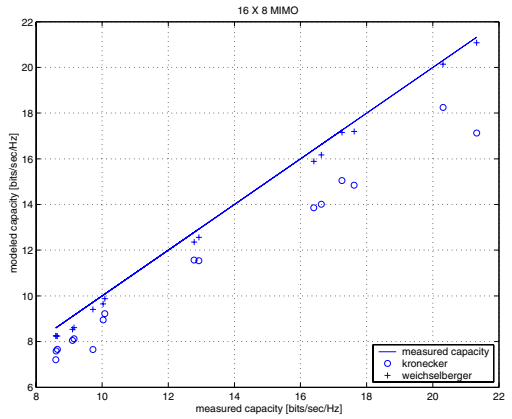

Fig. 9. NLOS, 16x8 MIMO; Scatter plot of average model capacity against average capacity of measured channel. The identity line indicates points of no modeling error.

where $\mathbf{H}(m)$ is the m :th channel realizaton. The Weichselberger model becomes the Kronecker model if and only if [7]

$$\Omega = \frac{1}{\sqrt{tr\{\mathbf{R}_{\mathrm{Rx}}\}}} \cdot \begin{bmatrix} \lambda_{\mathrm{Rx},1} \\ \lambda_{\mathrm{Rx},2} \\ \vdots \\ \lambda_{\mathrm{Rx},N_R} \end{bmatrix} \begin{bmatrix} \lambda_{\mathrm{Tx},1} \\ \lambda_{\mathrm{Tx},2} \\ \vdots \\ \lambda_{\mathrm{Tx},N_T} \end{bmatrix}^T, \qquad (9)$$

where $\lambda_{\mathrm{Rx},n_R}$ and $\lambda_{\mathrm{Tx},n_T}$ represent the eigenvalues of the correlation matrices at the receive and transmit side respectively. The coupling matrix in Eq. (9) has rank one. Figs. 8, 9 compare the modeled capacity with the Kronecker and measured one.

IV. Conclusions

Our analysis shows that the widely used assumption in channel modeling, that the channel can be represented as a sum of a weighted LOS component plus a zero-mean complex Gaussian distribution may not adequately represent measured data, i.e., shadow fading due to certain array configurations can distort the fading statistics of the chanel. In such scenarios, the Generalized Gamma distribution was found to best describe the behaviour of the measured chanel. We have highlighted the difference between the LOS power factor and the Ricean K-factor, in general the two quantities can have different values. We show that the DOA spectrum depends noticeably on the DOD, so the popular Kronecker model is not applicable. The performance of analytical channel models was evaluated by comparing the modeled channel capacity with the measured one. The Weichselberger model provided a better fit to the measured capacity as compared to the Kronecker model.

Acknowledgement 1: We would like to thank Prof. Larry Greenstein, Prof. Ernst Bonek, and the members of the COST 273 subworking group 2.1 for fruitful discussions. Part of this work was financed by an INGVAR grant of the Swedish Foundation for Strategic Research, and a grant from Vetenskapsradet.

References

[1] G. J. Foschini and M. J. Gans, "On limits of wireless communications in fading environments when using multiple antennas," *Wireless Personal Communications*, vol. 6, pp. 311–335, 1998.

[2] M. Steinbauer, A. F. Molisch, and E. Bonek, "The double-directional radio channel," *IEEE Antennas and Propagation Magazine*, pp. 51–63, August 2001.

[3] D. Gesbert, H. Blcskei, D. A. Gore, and A. J. Paulraj, "Outdoor MIMO wireless channels: models and performance prediction," *IEEE Transactions on Communications*, vol. 50, pp. 1926–1934, December 2002.

[4] P. Almers, F. Tufvesson, and A. F. Molisch, "Measurement of keyhole effect in a wireless multiple-input multiple-output (MIMO) channel," *IEEE Communications Letters*, vol. 7, pp. 373–375, August 2003.

[5] J. P. Kermoal, L. Schumacher, K. I. Pedersen, P. E. Mogensen, and F. Frederiksen, "A stochastic MIMO radio channel model with experimental validation," *IEEE Journal on Selected Areas in Communications*, vol. 20, pp. 1211–1226, August 2002.

[6] H. Özcelik, M. Herdin, W. Weichselberger, J. Wallace, and E. Bonek, "Deficiencies of the Kronecker MIMO radio channel model," *IEEE Electronics Letters*, vol. 39, pp. 1209–1210, August 2003.

[7] W. Weichselberger, H. Özcelik, M. Herdin, and E. Bonek, "A novel stochastic MIMO channel model and its physical interpretation," in *International Symposium on Wireless Personal Multimedia Communications, WPMC*, (Yokosuka, Japan), October 2003.

[8] S. Wyne, P. Almers, G. Eriksson, J. Karedal, F. Tufvesson, and A. F. Molisch, "Outdoor to indoor office MIMO measurements at 5.2 GHz," in *VTC 2004 - Fall*, (Los Angeles, USA), September 2004.

[9] B. H. Fleury, D. Dahlhaus, R. Heddergott, and M. Tschudin, "Wideband angle of arrival estimation using the SAGE algorithm," in *Proc. Spread Spectrum Techniques and Applications*, vol. 1, (Mainz), pp. 79–85, IEEE, September 1996.

[10] P. Soma, D. S. Baum, V. Erceg, R. Krishnamoorthy, and A. J. Paulraj, "Analysis and modeling of multiple-input multiple-output (MIMO) radio channel based on outdoor measurements conducted at 2.5 GHz for fixed BWA applications," in *Proc. ICC*, vol. 1, pp. 272–276, IEEE, April/May 2002.

[11] E. W. Stacy, "A generalisation of the Gamma function," *Annals of Mathematical Statistics*, vol. 33, pp. 1187–1192, 1962.

[12] J. Griffiths and J. McGeehan, "Interrelationship between some statistical distributions used in radio wave propagation," in *IEE Proc.*, vol. 129 part F, pp. 411–417, IEE, December 1982.

[13] L. J. Greenstein, D. G. Michelson, and V. Erceg, "Moment-method estimation of the Ricean K-factor," *IEEE Communications Letters*, vol. 3, pp. 175–176, June 1999.

[14] K. Yu, M. Bengtsson, B. Ottersten, D. McNamara, P. Karlsson, and M. Beach, "Second order statistics of NLOS indoor MIMO channels based on 5.2 GHz measurements," in *GLOBECOM 2001*, vol. 1, pp. 25–29, IEEE, 2001.

[15] E. Bonek, H. Özcelik, M. Herdin, W. Weichselberger, and J. Wallace, "Deficiencies of a popular stochastic MIMO radio channel model," in *International Symposium on Wireless Personal Multimedia Communications, WPMC*, (Yokosuka, Japan), October 2003.